Journal of Sound and Vibration 329 (2010) 96–108

Contents lists available at ScienceDirect

Journal of Sound and Vibration

journal homepage: www.elsevier.com/locate/jsvi

Subcomponent modelling of input parameters for statistical energy analysis by using a wave-based boundary condition

P. Ragnarsson [a,b,*], B. Pluymers [a], S. Donders [b], W. Desmet [a]

[a] K.U.Leuven, Department of Mechanical Engineering, Celestijnenlaan 300 B, B-3001 Heverlee, Belgium
[b] LMS International, Interleuvenlaan 68, B-3001 Leuven, Belgium

ARTICLE INFO

Article history:
Received 3 November 2008
Received in revised form
10 June 2009
Accepted 26 August 2009
Handling Editor: A.V. Metrikine
Available online 2 October 2009

ABSTRACT

This paper presents a new and efficient method to calculate point mobilities from subcomponents of a full structure. Subcomponent modelling is a commonly used method to gain information on the dynamic behaviour of complex assembly structures using smaller and more efficient models. For instance, point mobility calculations on subcomponent level are used to obtain more accurate input parameters for statistical energy analysis (SEA) models. A full system analysis is often too computationally expensive, so normally only individual subcomponents of the structure are extracted and analysed. This procedure yields a large reduction in computational effort, but also often results in a substantial loss of accuracy. This is due to the use of an approximation of boundary conditions to represent the eliminated remainder part of the structure, i.e. the full structure except the subcomponent at hand. Commonly, these boundary conditions are simplified by assuming clamped, free or simply supported edges. However, this is a huge simplification and may introduce large errors, especially in the low- and mid-frequency ranges. Earlier work has shown that a more accurate description of the boundary conditions can be achieved by describing the interface dynamics by a combination of so-called dynamic waves. In this paper, the method is developed further and a more robust and efficient wave extraction procedure is presented. An industrial body in white BIW is used as a test case and results are presented for three different cases. The results show that the wave-based boundary condition for point impedance calculations from a subcomponent model gives more accurate results than the results obtained with free or clamped boundary conditions.

1. Introduction

In modern vehicle design processes, the use of computer aided engineering (CAE) has increased dramatically in recent years. In order to reduce time to market and to minimise the number of prototypes for a vehicle manufacturer, it is crucial for a design engineer to get early and accurate predictions of the dynamic behaviour of new designs. Low-frequency methods such as the finite element method (FEM) [1] and the boundary element method (BEM) [2] have, thanks to increasing computer power, been able to run deterministic models to higher and higher frequencies, while statistical energy analysis (SEA) [3] has become the standard method for both acoustic and vibration analyses in the high-frequency range. However, there still exists a frequency gap for which no mature prediction method exists today [4]. In recent years,

* Corresponding author at: K.U.Leuven, Department of Mechanical Engineering, Celestijnenlaan 300 B, B-3001 Heverlee, Belgium. Fax: +32 16 32 29 87.
E-mail addresses: patrikragnarsson@hotmail.com, patrik.ragnarsson@mech.kuleuven.be (P. Ragnarsson).

0022-460X/$ - see front matter © 2009 Elsevier Ltd. All rights reserved.
doi:10.1016/j.jsv.2009.08.033

Nomenclature

E	time averaged energy
$\mathbf{f}$	element load vector (in FEM)
G	conductance (real part of mobility)
$\mathbf{K}$	FE stiffness matrix
$\mathbf{M}$	FE mass matrix
$n(\omega)$	modal density
$\mathbf{p}$	vector of wave participation factors
TF	transfer function
v	velocity
$\mathbf{V}$	WBS wave set
W	power
WTF	power transfer function
$\mathbf{x}$	vector of nodal displacement DOFs
Y	mobility
$\beta_{s,\mathrm{diss}}$	loss factor
$\beta_{s,r}$	reciprocal coupling factor
η_s	damping loss factor
$\eta_{s,r}$	coupling loss factor
φ	modal power
ω	angular frequency

research has focused on filling this gap by applying a number of different approaches. These approaches can be divided into three subcategories.

- Extending the applicable frequency range of the deterministic methods by improving the computational efficiency (automated multi-level substructuring, AMLS [5], fast multi-pole boundary element method (MPBEM) [6,7], Trefftz-based methods [8], etc.).
- Using standard FE solution schemes and postprocessing the results into SEA like quantities [9–11].
- Adding details to the SEA model by the use of finite element analysis (FEA) and enriching your SEA model with information from FE calculations or measurements [12–15].

This paper will focus on the third group of methods. One limiting factor for this group of methods is the calculation time for solving large FE models in the mid-frequency range. Another limitation is the loss of accuracy when only subcomponents are considered. This loss of accuracy depends on the selection of the boundary condition used at the interface of the subcomponent. Normally the interface dynamics are simplified by applying a free–free, clamped or simply supported boundary condition, which often is a too large simplification of the actual boundary condition. Therefore a method to improve the representation of the boundary condition for subcomponents is proposed. It will be shown that improving the representation of the boundary condition allows capturing the "true" behaviour of the component more accurately in a subcomponent model.

1.1. State of the art

Many previous papers have reported on combining deterministic methods and SEA in order to lower the applicable range of SEA. Langley and Bremner [16] developed a method based on partitioning the system into global and local degrees of freedom. The global problem was solved with normal deterministic methods and the local problem was solved using SEA equations. The method was further developed by Shorter and Langley [12], who developed a general method to predict ensemble average responses of complex systems by combining deterministic and statistical techniques. A coupled solution scheme was developed where the "stiff" components (long wavelength) are modelled with finite element (FE) and the "soft/flexible" components (short wavelength) are modelled with SEA. Deterministic information about the junctions between subcomponents is also taken into account. There are, however, still problems to be dealt with. For example, for each subsystem it must be decided whether the subsystem is "stiff" or "soft". This can either be done by using engineering experience or by performing a large number of subcomponent calculations to investigate whether a specific subsystem should be considered as "stiff" or "soft" [17,18]. Research is also targeting the possibility to combine finite element and periodic structure theory to add more detail to the SEA subsystems [17].

In classical SEA, the input parameters are normally evaluated using different analytical formulas that are valid for simple structures. This theory works well for high frequencies, but when trying to extend the use of SEA towards lower frequencies, other methods are needed. Lyon and DeJong [3] and later Manning [13,14] have shown that the point impedances at input and output locations can be used to better estimate the input power and the output response. This is a well-known method and for many years measurements have been used to obtain a better estimation of these parameters [19]. Lately the focus has been shifting more towards using FEM to calculate these important parameters. Mace et al. [10,20] presented a method to calculate the coupling loss factors in a robust way from FE analyses. Similar techniques have been used in other papers to improve the quality of other important SEA input parameters [15,25]. However, to run a complete FE calculation into the mid-frequency region is highly time consuming for industrial-sized models. To really capitalise on the strength of the deterministic methods, the calculation times must be reduced. One way to reduce the computational effort is to use subcomponent modelling in order to retrieve the important SEA parameters (input and

response point mobility, coupling loss factors (CLF), etc.) without having to run a calculation of the full model. A subcomponent can be any part of the complete model of interest. In vehicle analysis this can be for instance a B-pillar or a section of the floor panel. The goal is to run a fast calculation of a subcomponent and to retrieve a result that is as close as possible to the result one would expect from a calculation of the full model. Since the subcomponent is a part of a larger system, a dominant error source will be the boundary condition at the subcomponent interface. A classical way to treat this interface is to simplify the boundary conditions to a free or a fixed boundary condition [21]. As will be shown in this paper, this can work well for high frequencies (free BC) and for low frequencies (clamped BC), but for the mid-frequency range neither of these boundary condition types yields accurate results. Neither do any of these simplified boundary conditions perform well in the full frequency range. Therefore, improved methods are needed.

Wave-based substructuring (WBS) [22–24] is a substructuring method which uses a set of basis functions (waves) to describe the behaviour of the interfaces. In this paper a method to derive a boundary condition based on the wave-based substructuring technique is presented. First, a low-frequency WBS analysis is performed and the remaining structure (everything except the subcomponent) is reduced to a modal representation. This modal reduction of the remainder is then projected on the subcomponent via the set of previously calculated waves. As a next step, the low-frequency reduction of the remainder can be used as "boundary condition" for a subcomponent calculation at higher frequencies. The results are compared to results obtained in an analysis of a complete FE model of the same structure and with some commonly used boundary conditions.

1.2. Outline of the paper

To situate the presented method within the state of the art, Section 2 gives a brief introduction to SEA and discusses how the point mobility approach can be used to improve SEA models. Section 3 presents the theory behind conventional wave-based substructuring and describes how the method can be used to improve the boundary condition description for subcomponent analysis. In Section 4 three application cases are presented and the advantage of the wave-based boundary condition (as compared to free and clamped boundary conditions) is shown. The paper is concluded in Section 5.

2. SEA theory

2.1. Classical SEA

The analysis procedure using SEA is to divide the studied structure into structural and acoustic subsystems with a defined level of subsystem damping and coupling between the subsystems. The next step is to set up and to solve the power balance equation for these subsystems for one or more applied external power input excitations. The power balance equation for a subsystem s can be written as [3]

$$W_{s,\mathrm{in}} = W_{s,\mathrm{diss}} + \sum_{s \neq r} W_{s,r} \tag{1}$$

where $W_{s,\mathrm{in}}$ is the input power, $W_{s,\mathrm{diss}}$ is the power dissipated through damping mechanisms in subsystem s, and $W_{s,r}$ is the net power transmitted from subsystem s to subsystem r, ($W_{s,r} = -W_{r,s}$). For an SEA model with many subsystems this equation can be expressed in matrix form where the dissipated power and the transmitted power are expressed in terms of reciprocal coupling factors $\beta_{s,r}$, damping factors $\beta_{s,\mathrm{diss}}$ and modal powers φ_s [13,14,25]:

$$\begin{bmatrix} W_{1,\mathrm{in}} \\ W_{2,\mathrm{in}} \\ \vdots \end{bmatrix} = \begin{bmatrix} \beta_{1,\mathrm{diss}} + \sum_s \beta_{1,s} & -\beta_{1,2} & -\beta_{1,3} & \cdots \\ -\beta_{1,2} & \beta_{2,\mathrm{diss}} + \sum_s \beta_{2,s} & -\beta_{2,3} & \cdots \\ \vdots & \vdots & \ddots & \end{bmatrix} \begin{bmatrix} \varphi_1 \\ \varphi_2 \\ \vdots \end{bmatrix} \tag{2}$$

This matrix is limited-sized, and moreover symmetric and positive definite, so the computational advantages are obvious in terms of stability and solution speed. Besides this, there is an additional advantage that the coupling factors and the modal powers are parameters related to quantities that are easy to measure or calculate by FEA or other hybrid analysis methods. The use of reciprocal coupling factors $\beta_{s,r}$ (instead of coupling loss factors, CLF) is thus a key feature for the practical implementation of the SEA-FEA point mobility method described in the following section.

2.2. SEA-FEA point mobility approach

One frequently studied response in vehicle noise predictions is the transfer function (TF) from an excitation in one part of the vehicle to the response in another part of the vehicle. Important transfer functions in vehicle NVH are the structural transfer function from an applied force at an engine mount to the vibration of a floor panel and the structural–acoustic transfer function to the sound pressure level inside the car cabin near the driver's ear. The following equations are based on the formulations presented by Manning [13,14]. First, a dimensionless power transfer function WTF can be obtained by

defining a new term based on Eq. (2):

$$\mathrm{WTF}_{s,r} = \frac{\varphi_r}{W_{s,\mathrm{in}}} \tag{3}$$

where $\mathrm{WTF}_{s,r}$ is the power transfer function relating the modal power of the response subsystem r to the input power of the source subsystem s. However, in a typical vehicle development situation, the transfer function of interest is often the transfer function between the input force and the response velocity, which is also called the transfer mobility function:

$$\mathrm{TF}_{s,r} = \frac{v_r}{F_s} \tag{4}$$

This transfer mobility function $\mathrm{TF}_{s,r}$ can be written as a function of the SEA power transfer function $\mathrm{WTF}_{s,r}$ by expressing the input power as a function of the drive point conductance G_s (real part of the mobility) and the mean square of the applied force $\langle F_s^2 \rangle$. In classical SEA, the average subsystem conductance is used. The average is then taken over the spatial extent of the subsystem and over a band of frequencies. However, the relation shown in Eq. (5) can also be applied to single frequencies and to individual points as long as the proper conductance is used [13,14,26]:

$$W_{s,\mathrm{in}} = \langle F_s^2 \rangle G_s \tag{5}$$

The modal power φ_r can also be defined as a function of the drive point conductance G_r and the average mean square velocity $\langle v_r^2 \rangle$ of the subsystem:

$$\varphi_r = \frac{\pi}{2} \frac{\langle v_r^2 \rangle}{G_r} \tag{6}$$

Then the square of the transfer function between an input force in subsystem s and the response in subsystem r can be written as

$$|\mathrm{TF}_{s,r}|^2 = \frac{\langle v_r \rangle^2}{\langle F_s \rangle^2} = \frac{2 \cdot \varphi_r \cdot G_r}{\pi} \cdot \frac{G_s}{W_{s,\mathrm{in}}} = \frac{2}{\pi} \cdot G_s \cdot G_r \cdot \mathrm{WTF}_{s,r} \tag{7}$$

This very useful result gives an expression for the transfer mobility function based only on the power transfer function (SEA results) and the point conductance for both the excitation and the response point (which can be retrieved from measurement or FEA). It is also the basis for the point mobility approach presented in this paper and earlier reported in [13,14]. The point conductance calculations presented in this paper could be used to enhance the results from the SEA calculations and to enhance the quality of the coupling factors. The relation between coupling factors and point mobilities has also been shown by Manning:

$$\beta_{s,r} = \frac{1}{2\pi} \cdot \frac{4 \cdot G_s \cdot G_r}{|Y_s + Y_r|^2} \tag{8}$$

where Y is the complex valued point mobility and again subscript r and s refers to response and source, respectively. In classical SEA theory, the mobility functions are calculated from expressions for the infinite (or semi-infinite) system. The accuracy of this approach depends on the averaging bandwidth and the modal overlap factor. The modal overlap is a function of modal density and damping and the highest value is obtained when both of these parameters are large for a certain bandwidth. A wide bandwidth and/or high modal overlap result in a lower expected variance of the response from the mean prediction, so that a high accuracy of the result compared to a measurement is expected. This approach has shown to be a very accurate approximation for the high-frequency range where the modal overlap generally is high. This is the underlying reason that SEA has come to be accepted as the standard tool for high-frequency CAE analysis in vehicle design engineering. For the mid- and low-frequency ranges, where the modal overlap values tend to be smaller, the definition of the coupling factor in Eq. (8) using expressions for infinite systems may lead to large errors compared to measured response data [14]. The reason for this is that the smaller modal overlap is, the more the measured response (averaged over third octave bands) tends to depend on single deterministic phenomena.

By instead using FEA to calculate these point mobility functions, the transfer function accuracy can be improved for the mid- and low-frequency ranges. This can of course be performed using a full FE model of the investigated system, but if the system is large (for instance in the case of a car body in white (BIW) or a full vehicle model) the computational cost will prohibit to stretch the calculations towards higher frequencies. The point mobilities can also be calculated on only a part of the system [21]. Information about the boundary conditions for the interface between the remainder and the subcomponent must then be added to the model. Normally, free or clamped boundary conditions are applied, but this simplification will often lead to results in which some of the dynamic behaviour of the complete system are missed. The method that will be investigated in this paper is the use of a substructuring technique to capture the dynamic behaviour of the rest of the system. It will be investigated if a low-frequency substructuring calculation can be used as boundary condition for a subcomponent analysis in the mid- and high-frequency ranges. The substructuring scheme applied in this paper is the wave-based substructuring (WBS) technique [22–24]. The strength of this technique is that the number of interface DOFs is greatly reduced, which makes substructuring feasible even for structures with large interfaces. In Section 3, the theory of wave-based substructuring is explained.

3. Wave-based substructuring

Wave-based substructuring (WBS) is a powerful substructuring method in which the dynamic behaviour of the interfaces is described by a set of basis functions (waves). This reduces the model size compared to conventional substructuring methods as component mode synthesis (CMS) [27–29] as the number of waves needed to describe the dynamics of the interfaces is normally much smaller than the number of physical degrees of freedom (DOF) of the interfaces [22,23]. Instead of connecting the DOFs from two neighbouring subsystems directly via continuity equations, WBS connects two subsystems via a set of waves. The WBS continuity yields that the complete interface of the two subsystems can move only as a linear combination of a set of waves ($\mathbf{V}$) weighted by the wave participation factor ($\mathbf{p}$).

3.1. Theory

An undamped system with no external forces can be described by the FE matrix equation:

$$\mathbf{M}\ddot{\mathbf{x}} + \mathbf{K}\mathbf{x} = 0 \tag{9}$$

If this system is subdivided into non-overlapping substructures, the model can be divided into internal DOFs x_i and junction DOFs x_j. The equation of motion can then written as

$$\begin{bmatrix} \mathbf{M}_{ii} & \mathbf{M}_{ij} \\ \mathbf{M}_{ji} & \mathbf{M}_{jj} \end{bmatrix} \begin{bmatrix} \ddot{\mathbf{x}}_i \\ \ddot{\mathbf{x}}_j \end{bmatrix} + \begin{bmatrix} \mathbf{K}_{ii} & \mathbf{K}_{ij} \\ \mathbf{K}_{ji} & \mathbf{K}_{jj} \end{bmatrix} \begin{bmatrix} \mathbf{x}_i \\ \mathbf{x}_j \end{bmatrix} = \begin{bmatrix} 0 \\ \mathbf{f}_j \end{bmatrix} \tag{10}$$

In WBS, the junction DOFs are expressed as a linear combination of a set of waves ($\mathbf{V}$). These waves are weighted with a participation factor $\mathbf{p}$:

$$\mathbf{x}_j = \mathbf{V} \cdot \mathbf{p} \tag{11}$$

The equation of motion, Eq. (10), can then be written as

$$\begin{bmatrix} \mathbf{M}_{ii} & \mathbf{M}_{ij}\mathbf{V} \\ \mathbf{V}^T\mathbf{M}_{ji} & \mathbf{V}^T\mathbf{M}_{jj}\mathbf{V} \end{bmatrix} \begin{bmatrix} \ddot{\mathbf{x}}_i \\ \ddot{\mathbf{p}} \end{bmatrix} + \begin{bmatrix} \mathbf{K}_{ii} & \mathbf{K}_{ij}\mathbf{V} \\ \mathbf{V}^T\mathbf{K}_{ji} & \mathbf{V}^T\mathbf{K}_{jj}\mathbf{V} \end{bmatrix} \begin{bmatrix} \mathbf{x}_i \\ \mathbf{p} \end{bmatrix} = \begin{bmatrix} 0 \\ \mathbf{V}^T\mathbf{f}_j \end{bmatrix} \tag{12}$$

As in all substructuring methods, continuity and equilibrium conditions must be imposed at the boundaries. For a rigid connection between two subsystems (a) and (b), continuity of the interface displacement and equilibrium of the reaction forces are applied:

$$\mathbf{x}_j^{(a)} = \mathbf{x}_j^{(b)} \quad \text{and} \quad \mathbf{f}_j^{(a)} = \mathbf{f}_j^{(b)} \tag{13}$$

Transformed into a WBS framework, the continuity conditions will be

$$\mathbf{p}^{(a)} = \mathbf{p}^{(b)} \quad \text{and} \quad \mathbf{V}^T\mathbf{f}_j^{(a)} = \mathbf{V}^T\mathbf{f}_j^{(b)} \tag{14}$$

Only rigid connections are discussed in this paper. The theory for elastic connections has also been worked out, see Refs. [22,23].

3.2. WBS calculation procedure

A wave-based substructuring calculation procedure consists of two important calculation steps that differ somewhat from other substructuring techniques: the *wave calculation* and the *component reduction*. The assembly is divided into internal DOFs $\mathbf{x}_i$ and junction DOFs $\mathbf{x}_j$. The aim of the wave calculation is to calculate a matrix $\mathbf{V}$ such that the junction DOFs can be written as a linear combination of the waves according to Eq. (11).

The *wave calculation* procedure starts with the calculation of a full modal analysis of the complete structure in the frequency range of interest. The resulting modal matrix Φ can be projected onto the junction DOFs, so that the interface modal displacement matrix Φ_j is obtained. The individual modal vectors from the full modal analysis Φ are by definition orthonormal in the subspace of the entire structure. For the individual interface modal vectors Φ_j this is, however, not guaranteed. Two modes with very different displacement shape in another location could, by coincidence, have the same displacement shape at the interface. These two interface modal vectors will then be linear dependant. Therefore an orthonormalisation of these vectors must be performed, which aims at selecting the minimum number of vectors (waves) needed to represent the deformations at the subsystem interface.

To really capitalise on the strength of WBS, a *component reduction* of at least one of the components must be performed. WBS uses a variant of the conventional reduction procedure of MacNeal and Rubin [27,28] which consists of calculating the normal modes of the component in free–free conditions Φ' and the residual attachment modes Ψ' for each junction DOF (the suffix $'$ indicates that they are calculated in a WBS reduction procedure). The conventional reduction procedure is to apply a unit force to each interface DOF consecutively, keeping the other forces equal to zero. In WBS, a unit force "wave load vector" $\mathbf{V}^T\mathbf{f}_j$ is applied on one of the wave participation factors p, with zero forces on the other wave participation

factors. This is then repeated for all the wave participation factors. Physically this corresponds to applying a unit force to the entire interface with a distribution corresponding to the specific wave shape. If the number of wave participation factors **p** is smaller than the number of interface DOFs, a smaller number of residual attachment modes are needed to correctly represent the interface flexibility in assembly conditions, which thus reduces the calculation time. The WBS assembly can then be calculated by combining the waves, the reduced component and the parts kept as FE components.

3.3. Description of the "waves"

Starting from a modal analysis of the full FE model the displacement shapes at the substructure interface Φ_j can be defined. This set of displacement shapes is a limited set of basis functions that can be used to describe the structural dynamics of the interface. In a similar way, the "waves" are basis functions that allow the prediction of the interface dynamics in a specific frequency range. The waves have the following specification:

- The junction DOFs are expressed as a linear combination of a set of waves **V**, weighted by a participation factor **p**. The dimension of the wave matrix is hence $n_j^{\times} n_w$, with n_j the number of junction DOFs of the substructure and n_w the number of wave vectors in **V**.
- Since the waves are a projection of the orthonormal system modes on a subset of the system DOFs, orthonormality of the waves cannot be guaranteed. Therefore some post-processing of the waves is required, aiming at orthonormalisation of the waves and at selecting the minimum number of waves needed to represent the dynamics of the interfaces. For this purpose, one can use singular value decomposition (SVD) to decompose the interface modal displacement shapes into a set of orthonormal waves. The SVD also ranks the waves in order of importance for spanning the vector space of interest (i.e. in this case representing the interface dynamics). It is therefore straightforward to apply a threshold and to select the most relevant waves for the wave set.
- Since the wave calculation starts from a full assembly calculation, there is already some a priori knowledge of the interface dynamics of the complete system (in contrary to classical substructuring techniques).

In conventional WBS, the interface modal displacement shapes are obtained from a full FE analysis of the complete system. Research is ongoing to lower this requirement, for instance by obtaining the interface modal displacement shapes only from a smaller subassembly [30]. Furthermore, as will be described later in this paper, it is being investigated whether the interface modal displacement shapes from a calculation for a limited frequency range can be used instead. The waves and the reduced remainder from this low-frequency WBS analysis can then be used as boundary condition for an assembly analysis up to a much higher frequency range.

3.4. Validation example

3.4.1. Case description

Fig. 1 shows an industrial vehicle BIW model [23] (230 183 nodes, 223 323 elements) made of steel (Young's modulus $E = 210\,\text{GPa}$, Poisson coefficient $\nu = 0.3$, mass density $\rho = 7890\,\text{kg/m}^3$). The BIW consists of two rigidly connected substructures:

- The B-pillars (14 699 nodes and 13 697 elements).
- The body remainder (215 484 nodes and 209 328 elements).
- The connection consists of 298 junction nodes (i.e. 1788 junction DOFs).

WBS is applied in a B-pillar design scenario, and the performance and prediction accuracy are compared to classical substructuring according to MacNeal and Rubin [27,28]. All calculations have been performed on the same computer.

3.4.2. Results

The procedure in Section 3.2 is applied to create a WBS assembly of the B-pillars as full FE and the body remainder as a WBS-reduced modal model (as shown in Fig. 1d).

- A full FE modal analysis is performed in the range $[0, 100]$Hz; there are 35 modes (incl. 6 rigid body modes).
- An SVD orthonormalisation is performed; all 35 waves are kept. After the waves selection, the 35 wave participation factors are used for the interface representation (substituting 1788 junction DOFs).
- The BIW remainder is reduced using the procedure described in brief in Section 3.2 and more thoroughly in [22], by calculating the substructure modes up to 150 Hz and residual attachment modes only for the 35 wave participation factors.
- A rigid WBS connection is defined to create the WBS assembly.

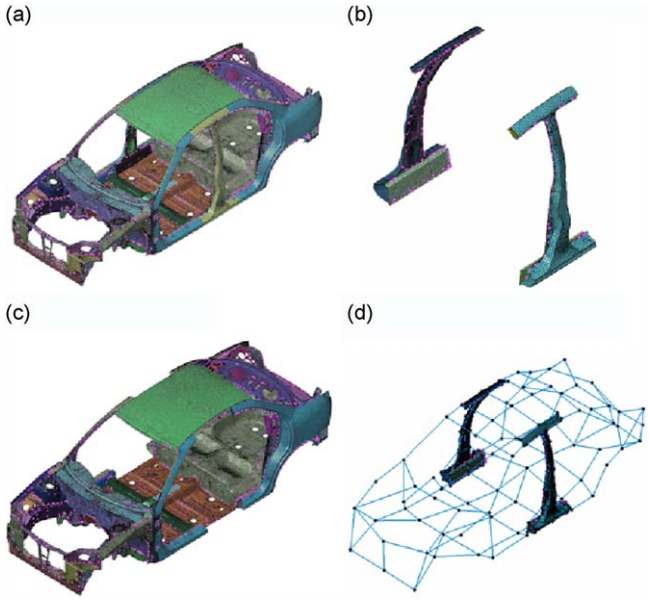

Fig. 1. Vehicle B-pillar case: industrial vehicle BIW FE model (a) consisting of two components: the B-pillars (b) and the body remainder (c). The reduced modal model of interest (d) has the B-pillars in FE representation and a reduced modal model for the vehicle BIW remainder. (a) Full FE model. (b) B-pillars component. (c) Body remainder component. (d) WBS-reduced assembly model.

Subsequently, also the conventional substructuring approach of MacNeal and Rubin [27,28] has been used to create a reduced assembly model as in Fig. 1d.

In Fig. 2, a comparison of the diagonal MAC values between the conventional substructuring technique (MacNeal, Rubin) and the WBS technique can be seen. The lowest MAC value for the conventional technique is 0.22906 and for WBS 0.999847. The CPU time for the reduction of the component is 54 min for WBS and 26 h 40 min for MacNeal–Rubin.

In summary, WBS offers a clear efficiency and accuracy benefit over the conventional MacNeal reduction procedure, especially for cases with large interface size between substructures. The reason for this is that WBS allows modelling the local flexibility at the interface with just a few enrichment vectors (here 35 compared to approximately 1800 for conventional CMS). It also brings some assembly-level behaviour into the interface description, which gives an increase of the accuracy of the method [23].

3.5. Using a WBS technique to derive boundary conditions for a subcomponent modelling approach

In this paper, it is investigated whether the WBS procedure can be used for subcomponent analysis in the mid- and high-frequency ranges. The idea is to perform a WBS calculation for the low- frequency range and to use this low-frequency information as boundary condition for a component calculation at much higher frequencies. In an FE scheme this is equivalent to constraining the interface DOFs (of the subcomponent) to move only as a linear combination of the waves extracted from the low-frequency WBS calculation. Fig. 3 outlines the calculation procedure used in this paper. The idea with this calculation procedure is to obtain a good and accurate boundary condition for the low-frequency range where the global behaviour of the structure is important for local point mobilities. At higher frequencies, where the dynamic behaviour of the subcomponent depends less on the global structure (it is "locally reacting"), information about the global behaviour is not that important to define the boundary condition.

4. Validation of the wave based boundary condition

As discussed in Section 1, a fast and accurate method to perform subcomponent modelling is crucial for using calculated point mobilities as a tool for evaluating the SEA parameters. In this section, it will be shown that the wave-based boundary condition, described above, has both these qualities. Three different test cases are presented and the point mobility functions of each test case are calculated using different techniques to simulate the boundary conditions. The results are then compared to a reference calculation consisting of a full FE calculation of the complete assembly (BIW) up to the frequency range of interest (700 Hz). For the new wave-based boundary condition to be successful, it has to be more accurate in the full frequency range than free and clamped boundary conditions and faster than a full assembly calculation.

(a)

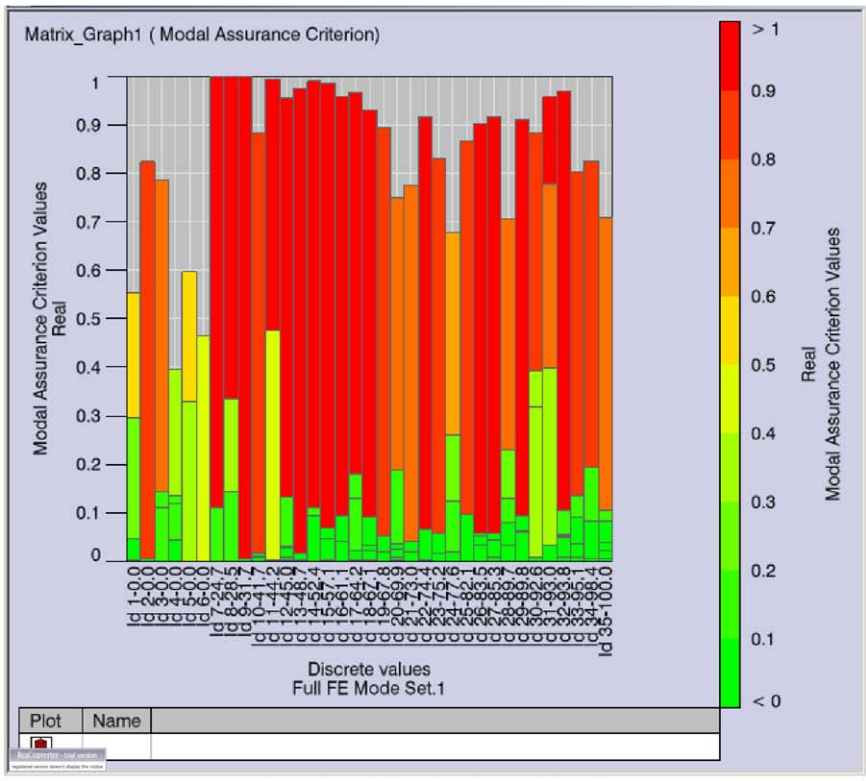

(b)

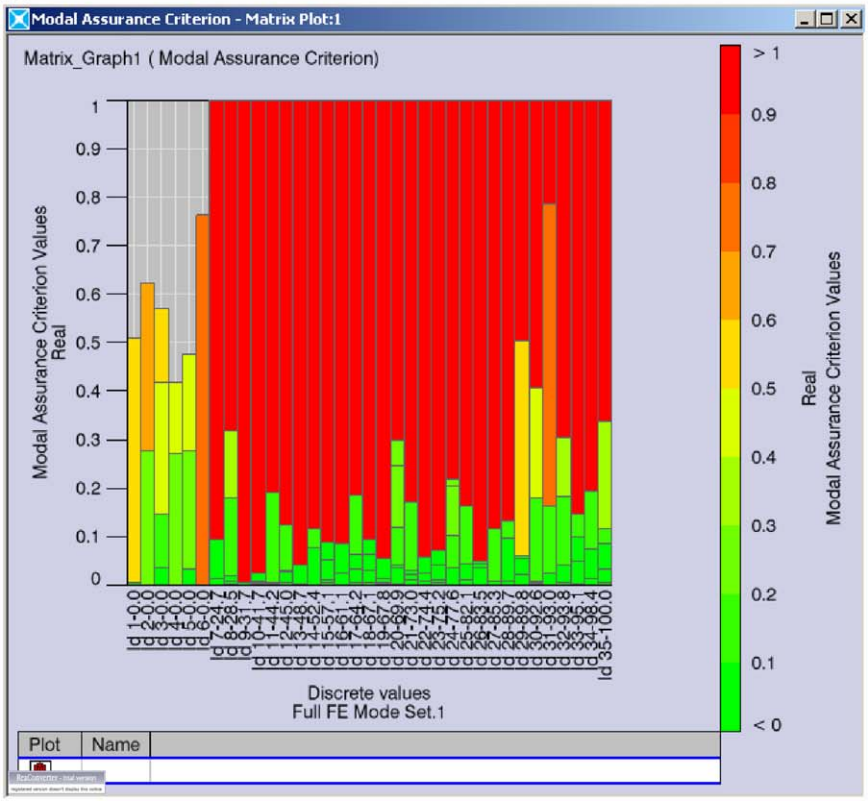

Fig. 2. Vehicle B-pillar case (see Fig. 1): side view if the MAC w.r.t. full FE results of MacNeal (a) and WBS (b).

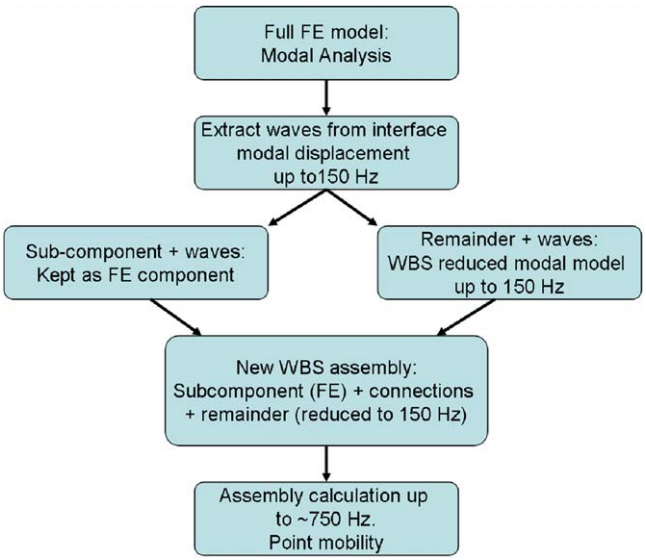

Fig. 3. Example of WBS calculation procedure used in this paper.

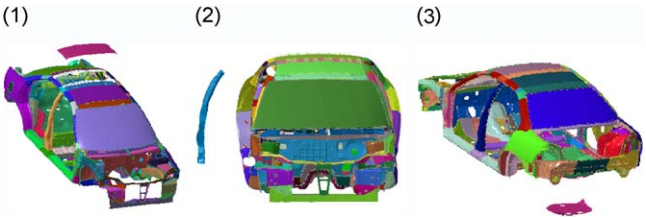

Fig. 4. The three different subcomponents considered in the paper, extracted from the full model for a clearer view. 1. Back of the roof, 2. B-pillar and 3. Spare wheel panel.

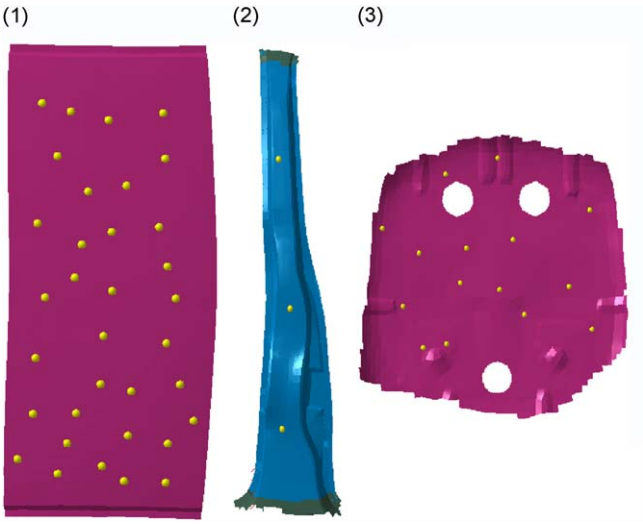

Fig. 5. The three different subcomponents considered in the paper, with the IO points marked with yellow dots. 1. Back of the roof (34 points), 2. B-pillar (3 points) and 3. Spare wheel panel (15 points). (For interpretation of the references to colour in this figure legend, the reader is referred to the web version of this article.)

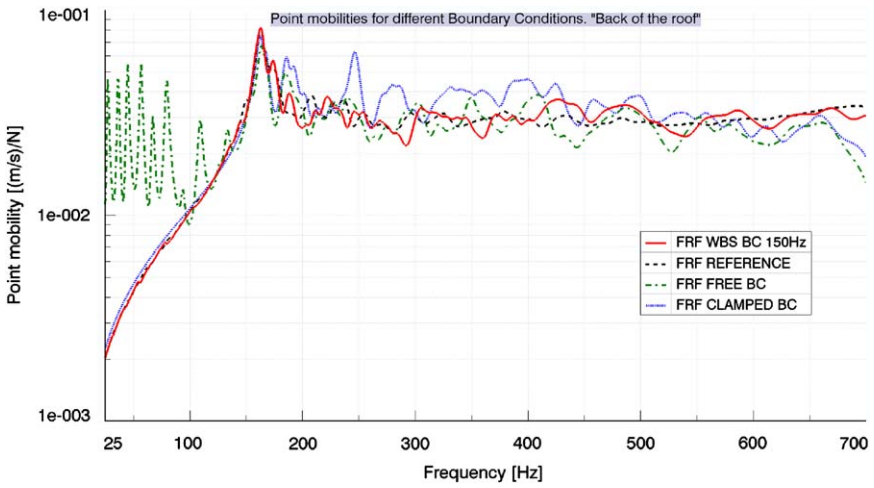

Fig. 6. Comparison of spatial averaged point mobilities for different boundary conditions for the back of the roof [(m/s)/N]. The reference result is a full assembly FE calculation.

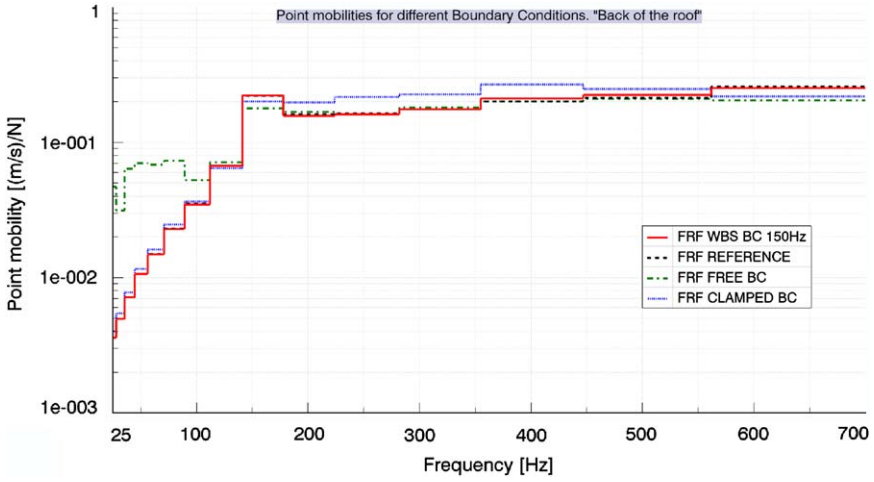

Fig. 7. Comparison of spatial and frequency averaged point mobilities for different boundary conditions for the back of the roof [(m/s)/N]. The reference result is a full assembly FE calculation.

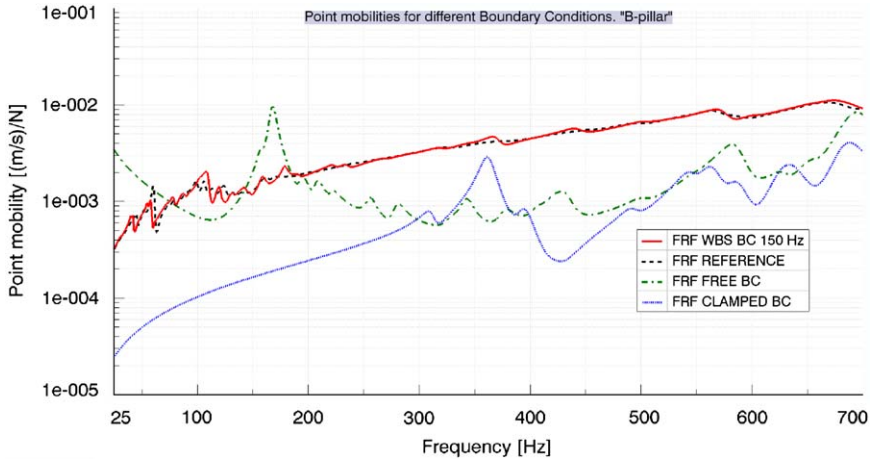

Fig. 8. Comparison of spatial averaged point mobilities for different boundary conditions for the B-pillar [(m/s)/N]. The reference result is a full assembly FE calculation.

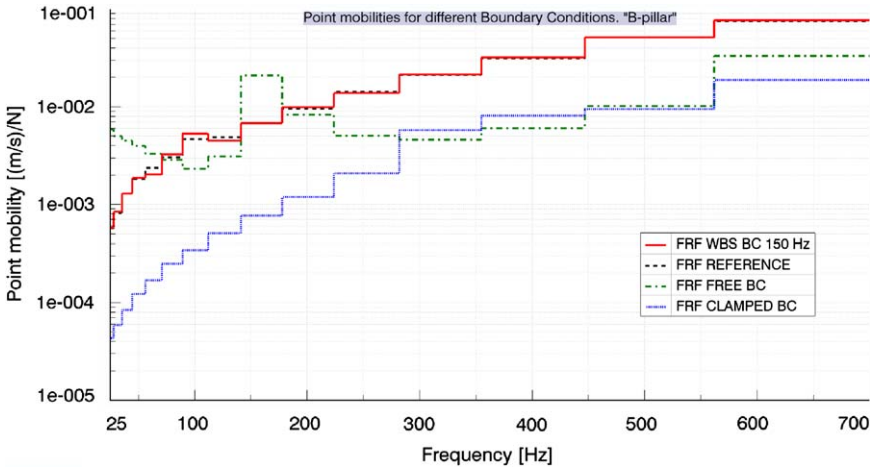

Fig. 9. Comparison of spatial and frequency averaged point mobilities for different boundary conditions for the B-pillar [(m/s)/N]. The reference result is a full assembly FE calculation.

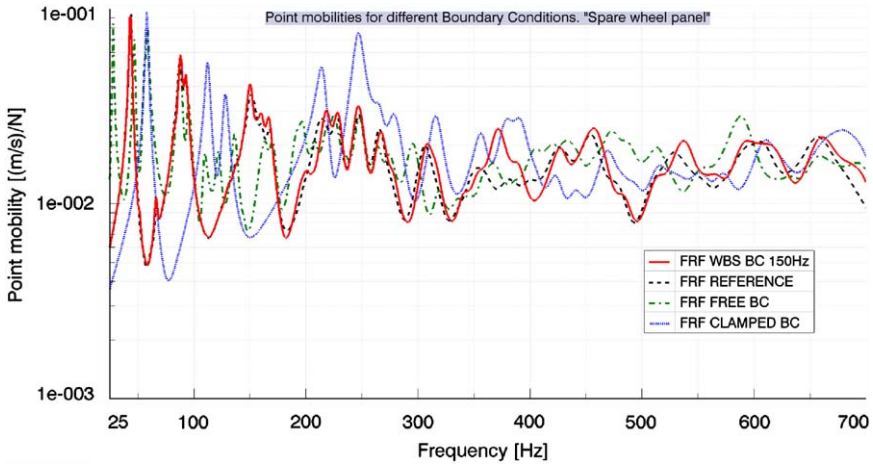

Fig. 10. Comparison of spatial averaged point mobilities for different boundary conditions for the spare wheel panel [(m/s)/N]. The reference result is a full assembly FE calculation.

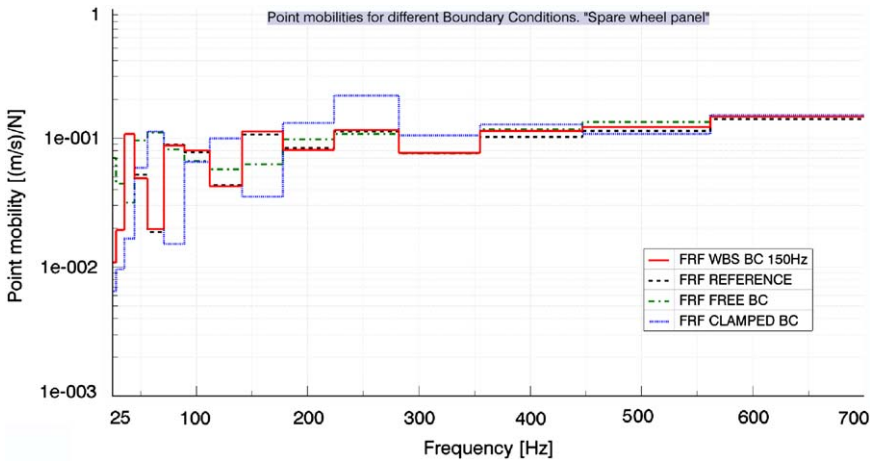

Fig. 11. Comparison of spatial and frequency averaged point mobilities for different boundary conditions for the spare wheel panel [(m/s)/N]. The reference result is a full assembly FE calculation.

The three investigated subcomponents are the back part of the roof, the B-pillar and a part of the spare wheel panel, see Fig. 4.

The model used in this paper is an industrial BIW containing 230 183 nodes and 223 323 elements. Different parts have been cut out from this model to allow simulating the different subcomponents. A modal analysis has been performed up to 700 Hz and an FRF synthesis has been performed based on the extracted modes. The FE calculation of the modes has been performed in MSC.Nastran 2004 [31]. The model setup, preprocessing, WBS definition, forced response analysis and postprocessing have been performed in LMS Virtual.Lab [32]. The response results have been averaged both over frequency (third octave bands) and spatially (average of the responses for all the IO points on the subcomponent, see Fig. 5).

4.1. Results

The results from the three test cases described above are presented in this section. For each case, the spatial average of the point mobility (velocity/force) at all IO points has been calculated. In Figs. 6–11 the results are shown both as narrow band (1 Hz) and as frequency averaged (third octave) results. As expected an almost perfect match between the wave-based boundary condition and the reference calculation can be seen for the frequency range where a full substructuring calculation (including a reduction of the remainder) has been performed [0–150 Hz]. For higher frequencies [>150 Hz], where the WBS reduction is not performed (but still used as boundary condition), the results are better than both free and clamped boundary conditions. It can also be seen that the free boundary condition gives inaccurate results for the low-frequency region and that the clamped boundary condition has the overall worst performance at high frequencies. It can also be seen that the wave-based boundary condition seems to work well for all three different types of test cases. While the free and clamped boundary conditions clearly show its limitations for test case 2. Here the influence from the rest of the assembly is big and since no information from the assembly is included in the free or clamped boundary conditions, the true behaviour of the structure cannot be captured. With the wave-based boundary condition, however, some assembly level information is already included in the boundary condition and the point mobility calculation is much more accurate.

5. Conclusions

As can be seen in the results in Section 4, the calculations with the wave-based boundary condition show, as expected, an almost perfect match to the reference calculation up to 150 Hz. This is the frequency up to which the wave extraction and the reduction has been performed. For higher frequencies (150–700 Hz), a region for which no dynamic waves have been obtained, the results are still good. In this frequency range the WBS reduction obtained from the low-frequency calculations is used as boundary conditions (boundary constraints). Since the subcomponents tend to be more and more locally reacting for higher frequencies, the applied boundary condition is less important for higher frequencies. In general, the results from the calculations with the wave-based boundary condition are better than the results from calculations with either free or clamped boundary conditions. Furthermore, the computational cost for performing calculations with the wave-based boundary condition is much smaller than for a full FE calculation of the complete assembly. In WBS, two "large" calculations are needed. First, a full FE analysis of the assembles system must be performed, followed by a reduction calculation of the remainder. However, if the frequency limit for these two calculations can be kept low (here 150 Hz), the time consumption will be much less than for one full assembly FE analysis up to 700 Hz. Using free or clamped boundary conditions instead would of course be much faster, but as has been shown in the calculations presented above, the accuracy is not always good enough.

Future work will focus on exploring the possibilities to make the calculation procedure even more efficient, either by lowering the required frequency limit for the wave-based boundary condition calculations or by exploring faster ways to perform the "larger" WBS calculations. Automated multi-level substructuring (AMLS) [33] will be explored for this purpose.

Acknowledgements

We kindly acknowledge IWT Vlaanderen for their support of the Project IWT-070337 MIDAS—next generation numerical tools for mid-frequency acoustics, and we gratefully acknowledge the European Commission for their support of the Collaborative Project CP-218508 MID-MOD—mid-frequency vibro-acoustic modelling tools. Furthermore, we kindly acknowledge the European Commission for their support of the Marie Curie EST Project SIMVIA2 (http://www.simvia2.eu,contract nr. MEST-CT-2005-020263), from which Mr. Patrik Ragnarsson holds a Research Training grant. Finally, Bert Pluymers wishes to acknowledge the Industrial Research Fund K.U.Leuven.

References

[1] O.C. Zienkiewicz, R.L. Taylor, J.Z. Zhu, P. Nithiarasu, *Finite Element Method—The Three Volume Set*, Sixth ed., Butterworth-Heinemann, Boston, 2005.
[2] O. Von Estorff, *Boundary Elements in Acoustics: Advances and Applications*, WIT Press, 2000.
[3] R.H. Lyon, R.G. DeJong, *Theory and Application of Statistical Energy Analysis*, Second ed., Butterworth-Heinemann, Boston, 1995.

[4] W. Desmet, Mid-frequency vibro-acoustic modelling: challenges and potential solutions, *Proceedings of ISMA 2002*, Leuven, Belgium, 2002, pp. 835–862.
[5] J.K. Bennighof, R.B. Lehoucq, An automated multilevel substructuring method for eigenspace computation in linear elastodynamics, *SIAM Journal on Scientific Computing* 25 (6) (2004) 2084–2106.
[6] M. Fischer, U. Gauger, L. Gaul, A multipole Galerkin boundary element method for acoustics, *Engineering Analysis with Boundary Elements* 28 (2004) 155–162.
[7] Y. Yasuda, T. Sakuma, Fast multipole boundary element method for large-scale steady-state sound field analysis. Part II: Examination of numerical items, *Acta Acustica united with Acustica* 89 (2003) 28–38.
[8] B. Pluymers, B. Van Hal, D. Vandepitte, W. Desmet, Trefftz-based methods for time-harmonic acoustics, *Archives of Computational Methods in Engineering* (2007) 343–381.
[9] A. Carcaterra, Ensemble energy average and energy flow relationships for nonstationary vibrating systems, *Journal of Sound and Vibration* 288 (3) (2005) 751–790.
[10] B.R. Mace, P.J. Shorter, Energy flow models from finite element analysis, *Journal of Sound and Vibration* 233 (3) (2000) 369–389.
[11] N. Vlahopoulos, X. Zhao, T. Allen, An approach for evaluating power transfer coefficients for spot-welded joints in an energy finite element formulation, *Journal of Sound and Vibration* 220 (1) (1999) 135–154.
[12] P.J. Shorter, R.S. Langley, Vibro-acoustic analysis of complex systems, *Journal of Sound and Vibration* 288 (3) (2005) 669–699.
[13] J.E. Manning, Formulation of SEA parameters using mobility functions, *Philosophical Transactions of the Royal Society of London, Series A: Physical and Engineering Sciences* 346 (1681) (1994) 477–488.
[14] J.E. Manning, Use of measured mobility to improve SEA predictions in the mid-frequency range, *Proceedings of DETC99*, Las Vegas, NV, USA, 1999, September 12–15.
[15] G. Borello, L. Gagliardini, Virtual SEA: towards an industrial process, *SAE Noise and Vibration Conference Proceedings*, Number 2007-01-2302, St. Charles, IL, 2007.
[16] R.S. Langley, P. Bremner, A hybrid method for the vibration analysis of complex structural–acoustic systems, *Journal of the Acoustical Society of America* 105 (3) (1999) 1657–1671.
[17] V. Cotoni, R.S. Langley, P.J. Shorter, A statistical energy analysis subsystem formulation using finite element and periodic structure theory, *Journal of Sound and Vibration* 318 (2008) 1077–1108.
[18] A. Charpentier, V. Cotoni, K. Fukui, Using the hybrid FE-SEA method to predict structure-borne noise in a car body-in-white, *Proceedings of Internoise 2006*, Honolulu, HI, 2006, December 3–6.
[19] J.E. Manning, SEA models to predict structureborne noise in vehicles, *SAE Noise and Vibration Conference Proceedings*, 2003-01-1542, 2003.
[20] A.N. Thite, B.R. Mace, Robust estimation of coupling loss factors from finite element analysis, *Journal of Sound and Vibration* 303 (2007) 814–831.
[21] J.E. Manning, Hybrid SEA for mid-frequencies, *SAE Noise and Vibration Conference Proceedings*, number 2007-01-2305, St. Charles, IL, 2007.
[22] S. Donders, B. Pluymers, P. Ragnarsson, R. Hadjit, W. Desmet, The wave-based substructuring approach for the efficient description of interface dynamics in substructuring, *Journal of Sound and Vibration* (2009), submitted for publication (under review).
[23] S. Donders, Computer-aided Engineering Methodologies for Robust Automotive NVH Design, PhD Thesis, K.U.Leuven, Department of Mechanical Engineering, Division PMA, Leuven, Belgium, February 2008. Available online: 〈http://hdl.handle.net/1979/1698〉.
[24] S. Donders, R. Hadjit, K. Cuppens, M. Brughmans, W. Desmet, A wave-based substructuring approach for faster vehicle assembly predictions, *Proceedings of NOVEM 2005*, Saint-Raphaël, France, 2005, April 18–21.
[25] P. Ragnarsson, K. De Langhe, J. Betts, C.T. Musser, Using FE analysis to improve SEA at mid-frequencies, *Proceedings of Internoise 2007*, Istanbul, Turkey, 2007, August 28–31.
[26] J.E. Manning, SEA: a practical NVH design analysis method, *Proceedings of the Styrian Noise, Vibration and Harshness Congress*, Graz, Austria, November 15–17, 2006, pp. 123–132.
[27] R.H. MacNeal, A hybrid method of component mode synthesis, *Computers & Structures* 1 (4) (1971) 581–601.
[28] S. Rubin, Improved Component-Mode Representation for Structural Dynamic Analysis, *AIAA Journal* 13 (8) (1975) 995–1006.
[29] R.R. Craig Jr., M.C.C. Bampton, Coupling of substructures for dynamic analyses, *AIAA Journal* 6 (7) (1968) 1313–1319.
[30] P. Cermelj, W. Desmet, S. Donders, B. Pluymers, M. Boltezar, Basis functions and their sensitivity in the wave-based substructuring approach, *Proceedings of ISMA 2008*, Leuven, Belgium, September 15–17, 2008.
[31] MSC. MSC Nastran 2004, 2004.
[32] LMS International. LMS Virtual.Lab Rev 8A-SL1, 2008.
[33] J.K. Bennighof, M.F. Kaplan, M.B. Muller, M. Kim, Meeting the NVH computational challenge: automated multi-level substructuring, *Proceedings of the International Modal Analysis Conference XVIII (IMAC18)*, San Antonio, USA, 2000.